Article

Journal of
Nanoscience and Nanotechnology
Vol. 19, 991–995, 2019
www.aspbs.com/jnn

1,3,5-Trinitrotoluene Sensor Based on Silole Nanoaggregates

Bomina Shin and Honglae Sohn*

Department of Chemistry, Chosun University, Gwangju 501-759, Korea

Bis(methyltetraphenyl)silole and bis(methyltetraphenyl)silole siloxane nanoaggregates for the detection of TNT were developed by using aggregation-induced emission property. Their absolute quantum yields and critical water concentration for onset of aggregation were measured. Average particle size for both nanoaggregates were measured and tuned by controlling the water fraction by volume. Absolute quantum yield of both nanoaggregates in 90% water volume fraction increased by more than 40 times. Detection of TNT was achieved from the quenching PL measurement of both nanoaggregates by adding the TNT. A linear Stern–Volmer relationship was observed for the detection of TNT.

Keywords: Sensor, Explosive, Silole, Aggregate, Quenching.

1. INTRODUCTION

Materials with high emission are very intriguing and highly demanded in optical and electronic devices. Previously developed materials with known fluorescent molecules exhibited high fluorescence in dilute solution exhibit low or no emission in the solid state, because the strong intermolecular $\pi-\pi$ stacking interaction causes an aggregation-caused emission quenching (ACEQ).[1] The ACEQ is generally attributed to a nonradiative deactivation process, such as excitonic coupling, excimer formation, and excitation energy migration to the impurity traps.[2,3] Since the most of the fluorescent molecules are donor–acceptor type or flat π-conjugated molecules, they are more prone to molecular aggregation and fluorescence quenching in the solid state.[4,5]

Decrease of emission efficiency in the solid state has been a major problem in optical device applications. Many attempts through chemical, physical, and engineering approaches have been made to prevent the formation of less emissive species. To overcome this problem, an aggregation-induced emission enhancement (AIEE) is an alternative approach is to control the fluorescence properties in the solid state. Recently, many aromatic AIEE compounds have been reported.[6]

Siloles have recently attracted much attention due to its unique electronic properties.[7,8] The unique optical and electrical phenomenon could be applied in various fields, such as electron transporting materials,[9] light-emitting diodes (LEDs),[10–12] chemical sensors,[13,14] and flexible memory storage.[15] Siloles is structured with π-electron systems containing Si atom as a part of cyclic 5-membered ring that shows an AIEE.[16] These non-emissive molecules are induced to be efficiently emissive by aggregate formation. The above effect of aggregation shows opposite behavior from the one observed in common luminophore systems, where aggregate formation usually cause decrease in PL efficiency. On the other hand, nanoaggregate has a surprising increase in PL efficiency when it nanoaggregates in water.[17–19] AIEE has been attributed by the restricted rotation of the phenyl rings, which limits the nonradiative decay pathways.[20]

Sensors offering new approaches to the rapid detection of ultra-trace anaytes from explosives, have attracted attention because explosives are important chemical species to detect in mine fields, forensic investigations, and homeland security applications. Silole have also been shown to have potential as chemo-sensors for detecting explosives.[14] Because explosives such as 1,3,5-trinitrotoluene (TNT) are electron deficient compounds due to nitro moiety in a molecule, photoluminescence (PL) of silole decreases via electron transfer quenching.

Herein, we report synthesis and optical characterization of two different types of silole fluorophore nanoaggregates such as silole nanoaggregate and silole-siloxane

*Author to whom correspondence should be addressed.

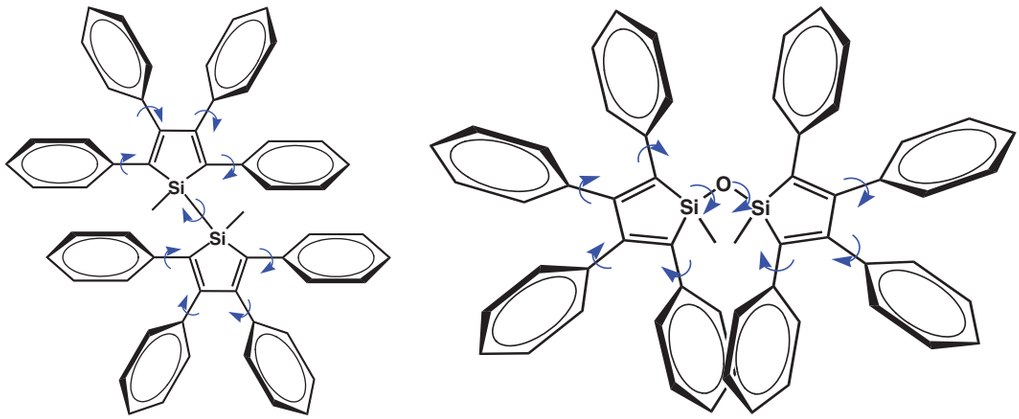

Figure 1. Chemical structure of bis(methyltetraphenyl)silole (left) and bis(methyltetraphenyl)silole siloxane (right).

nanoaggregate. Evidently, those nanoaggregates showing high PL efficiency through AIEE, would have the high efficiency in sensing explosives. An AIEE of silole and silole-siloxane nanoaggregates and their Stern–Volmer analyses for the comparison of the detection efficiencies of explosives are reported.

2. EXPERIMENTAL DETAILS

2.1. General

All synthetic manipulations were carried out under an atmosphere of dry argon gas using standard vacuum-line Schlenk technique. All solvents were purified and degassed before use according to standard literature methods: diethylether, tetrahydrofuran (THF), *n*-Hexane, ethanol were purchased from Aldrich Chemical Co. Inc. and distilled from sodium/benzophenone ketyl. All other reagents (Aldrich) such as diphenylacetylene, lithium wire, and methyltrichlorosilane were purchased and used without any purification. Spectroscopic grade THF from Fisher Scientific was used for the fluorescence measurements. The concentration of silole nanoaggregates for the fluorescence measurement was 10 mg/100 mL.

2.2. Preparation of Bis(methyltetraphenyl)Silole

The preparation method of bis(methyltetraphenyl)silole was previously reported.[21]

2.3. Preparation of Bis(methyltetraphenyl) Silole Siloxane

To a solution of 1-chloro-1-methyl-2,3,4,5-tetraphenyl-1-silacyclopentadiene (4.58 g, 10 mmol) in THF (200 mL) was added H_2O (0.18 g, 10 mmol) and triethlyamime (1.01 g, 10 mmol). After stirred at room temperature for 24 hrs. After evaporating THF from the mixture, the remaining solid was treated with water and diethylether. The organic layer was separated and dried ($MgSO_4$). The solvent was removed *in vacuo*, and the solid was washed with ethanol for purification.[24]

Mp ≥250 °C. ^{1}H NMR (300 MHz, $CDCl_3$ (δ 7.26)): δ 6.7–6.8 and 6.9–7.2 (m, 40H, Ph), 0.38 (s, 6H). ^{13}C NMR (100 MHz, CD_2Cl_3 (δ 77.00)): δ 154.6, 139.07, 138.81, 137.34, 130.16, 129.53, 128.54, 128.08, 126.99, 126.46, −2.7.

2.4. Instruments and Data Acquisitions

Fluorescence emission spectrum were recorded with the use of a Perkin-Elmer luminescence spectrometer LS 50B. The solvents were determined to be free of emitting impurities prior to use. To avoid changing the concentrations of the emitting compound, the experiments were carried out with solution by preparing the quencher in the same solution of the emitting compound. Absolute PL quantum yield (QY) was obtained by using a Quantaurus-QY Absolute PL quantum yield spectrometer C11347-11

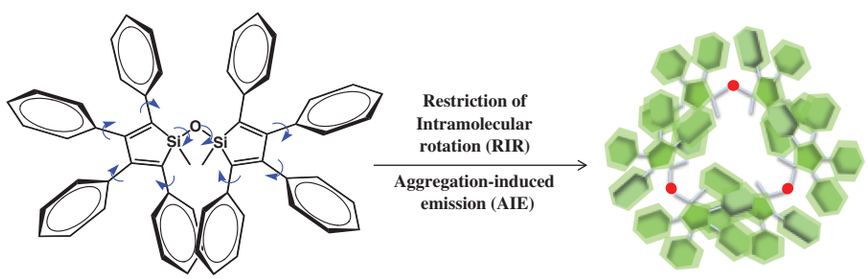

Figure 2. Schematic diagram for the preparation of silole nanoaggregates.

(Hamamatsu, Japan) with of 150 W xenon monochromatic light source, multichannel Czerny-Turner type spectroscope, and 3.3 inch spectral on integrating sphere. Dynamic light scattering (DLS) measurement was conducted by employing a DLS-8000HL (Otsuka Electronics, Japan) with 10 mW He–Ne Laser (Max 30 mW), photomultiplier tube detector, and silicon photodiode monitor detector.

3. RESULTS AND DISCUSSION

Siloles have attracted attention because of their unusual electronic and optical properties caused from extensively delocalization through silicon atom of five membered ring at LUMO level. Silole have also been shown to have potential as chemo-sensors for detecting explosives.[14] One of the characteristic optical property of silole is AIEE. AIEE is result from the steric effect of the peripheral phenyl rings caused nonplanar conformations, which prevents them from packing via $\pi-\pi$ stacking interactions and quenching by excimers. The restriction of intramolecular rotations in the aggregates blocks the nonradiative decay, hence changing the weak emitters to strong emitters.

Two different types of nanoaggregates containing silole molecules, silole nanoaggregate and silole-siloxane nanoaggregate were provided and examined for their optical properties in nanoaggregates. Figure 1 shows the molecular structures and intermolecular rotations. In case of bis(methyltetraphenyl)silole, two silole units are directly connected through Si–Si bond which could cause more strict intramolecular rotation and conjugation of silicon σ bond. However, two silole units in bis(methyltetraphenyl)silole siloxane are connected by oxygen atom, which allows more flexible intramolecular rotation.

Bis(methyltetraphenyl)silole and bis(methyltetraphenyl) silole siloxane show emission near 490 and 480 nm, when excited at 360 nm, respectively. Absolute quantum yield (QY) of bis(methyltetraphenyl)silole and bis(methyltetraphenyl)silole siloxane are measured in THF solution and exhibits 0.8% and 0.4%, respectively. This result might be due to the short conjugation of silole unit through Si–Si bond. To prepare the nanoaggregates, the mother solution was prepared by dissolving 10 mg of silole in 100 mL THF. The silole nanoaggregates were prepared by rapid injection of 1 mL silole solution into a different proportions ratios of THF and distilled water such as THF:H_2O = 0:9, 1:8, 2:7, and so forth. Schematic diagram for the preparation of silole nanoaggregates is shown in Figure 2.

Figure 3(A) shows the relative PL spectra of bis(methyltetraphenyl)silole nanoaggregate in water-THF mixtures (% water from top; 90%, 80%, 70%, 60%, 50%, 40%, 30%, 20%, 10%, 0%). Figure 3(B) shows the relative PL spectra of bis(methyltetraphenyl) silole siloxane nanoaggregate in water-THF mixtures. Figure 3(C) shows the PL efficiency of bis(methyltetraphenyl)silole nanoaggregate versus % water by volume. Bis(methyltetraphenyl)silole nanoaggregate

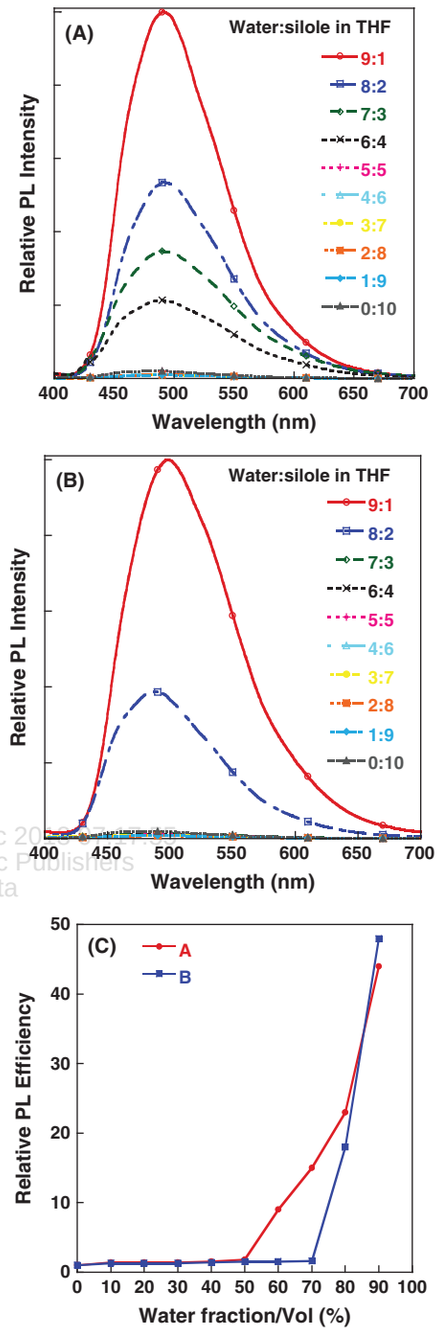

Figure 3. PL spectra of bis(methyltetraphenyl)silole (A) and bis(methyltetraphenyl)silole siloxane (B) nanoaggregates in water-THF mixtures (% water from top; 90%, 80%, 70%, 60%, 50%, 40%, 30%, 20%, 10%, 0%). Plot of the relative intensity of bis(methyltetraphenyl)silole nanoaggregate (red) and bis(methyltetraphenyl)silole siloxane nanoaggregate (blue) versus % water by volume (C).

exhibits a nearly identical emission band, however the emission band of bis(methyltetraphenyl)silole siloxane nanoaggregates red-shifts by 20 nm in nanoaggregates. For bis(methyltetraphenyl)silole solution in pure THF, the PL is very weak near 490 nm. In solutions between 0% and 50% water by volume, the PL efficiency of bis(methyltetraphenyl)silole nanoaggregates does not increased. However, the PL efficiency increases over 50% water by volume, which indicates the onset of aggregation. In case of bis(methyltetraphenyl)silole siloxane nanoaggregate, the PL efficiency increases over 70% water by volume. As the water fraction is increased, the PL efficiency increases dramatically. Critical water concentration for the formation of bissilole and bissilole siloxane nanoaggregate are a minimum volume-fraction of 50% and 70% water, respectively. Since AIEE is due to result from the steric effect and the restriction of intramolecular rotations in the aggregates, more strict intramolecular rotation of bissilole exhibits lower % water of the onset of aggregation. Absolute quantum yield of bissilole and bissilole siloxane nanoaggregates in 90% water volume fraction were 32.4% and 18.7%, respectively. The PL efficiencies for both nanoaggregates increased more than 40 times.

Figure 4, obtained by dynamic light scattering measurements shows the size of nanoaggregate and size distribution in different water fractions. Particle diameter decreases as water fraction increases, but the dispersity of diameter for given any suspension is about ±3%. Both nanoaggregates exhibit a minimum in size at 90% water. Average particle diameters for

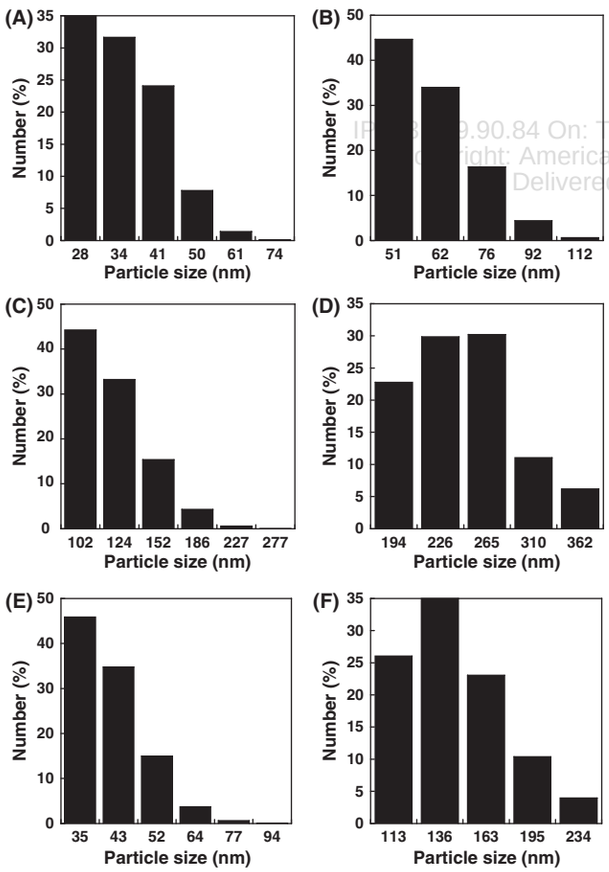

Figure 4. DLS data showing an increase in size when the water fraction ratio decreases to 90% (A), 80% (B), 70% (C), and 60% (D) for bis(methyltetraphenyl)silole nanoaggregate and 90% (E) and 80% (F) for bis(methyltetraphenyl)silole siloxane nanoaggregate.

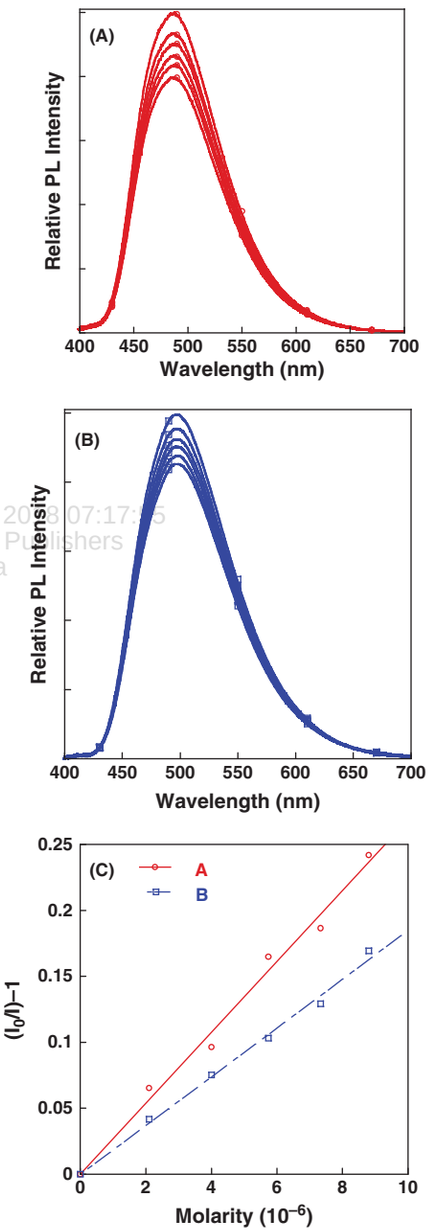

Figure 5. Quenching PL spectra of increasing fraction by 500 part per billion (ppb) of each TNT concentration in bis(methyltetraphenyl)silole nanoaggregates solution (A) and bis(methyltetraphenyl)silole siloxane nanoaggregates solution (B). Stern–Volmer plot showing sensing efficiency for both nanoaggregates (C).

the bis(methyltetraphenyl)silole nanoaggregate are 35, 60, 110, 260 nm as the water volume fraction decreases 90 to 60%, respectively. (See Figs. 4(A to D)). Average particle diameters for the bis(methyltetraphenyl)silole siloxane nanoaggregate are 39 and 130 nm as the water volume fraction decreases 90 to 80%, respectively. (See Figs. 4(E to F)) Decrease of particle size at higher water concentrations could be explained that the hydrophobic organic molecules are prone to aggregate to a higher extent in the hydrophilic environment.

The ability of the silole nanoaggregate with a volume-fraction of 90% water to detect TNT through PL quenching was investigated by adding successive aliquots of an identical volume-fraction of 90% water stock solution of TNT to the nanoaggregate. Figures 5(A) and (B) show quenching PL spectra of increasing fraction by 500 part per billion (ppb) of each TNT concentration in both silole nanoaggregates solution. The decrease in PL was monitored as a function of added TNT. The responses to quenching between both silole nanoaggregates were analyzed using the Stern–Volmer equation:[22] $I_0/I = K_{SV}[Q]+1$. In this equation, I is the fluorescence intensity at quencher concentration, $[Q]$, I_0 is the intensity at $[Q]=0$, and K_{SV} is the Stern–Volmer constant. Linear Stern–Volmer relationships are observed for both nanoaggregates.

Stern–Volmer constant (K_{SV}) of bis(methyltetraphenyl) silole nanoaggregates and bis(methyltetraphenyl)silole siloxane nanoaggregates for TNT were 26,000 and 18,000 M^{-1}, respectively. Previously we reported that the Stern–Volmer constant of non-aggregate silole polymer, poly(tetraphenyl)siloles, for TNT detection was about 4,350 M^{-1}.[14] Trogler et al reported that the Stern–Volmer constant of oligo(tetraphenyl)silole nanoaggregate with a volume-fraction of 90% water was 4,100 M^{-1}.[23] Thus, the detection efficiency of bis(methyltetraphenyl)silole nanoaggregates in the water fraction of 90% for TNT increased by about 4 to 5 times compared to that of previous reported value. Higher detection efficiency of bis(methyltetraphenyl)silole nanoaggregates could be result from the conjugation through Si–Si bond between silole units.

4. CONCLUSION

Aggregation-induced emission properties of conjugated silole nanoaggregates and non-conjugated silole siloxane nanoaggregates and their successful sensing of explosive were reported. Both silole nanoaggregates exhibited an aggregation-induced emission enhancement of more than 40 times increase to normal photoluminescence when the water fraction was increased to 90%. Both silole nanoaggregates used for the detection of TNT and showed greater sensitivity compared to previously reported value.

Acknowledgment: This research was financially supported by the Agency for Defense Development and the National Research Foundation of Korea (NRF) funded by the Ministry of Education (NRF-2016R1D1A1B03933216).

References and Notes

1. G. M. Fischer, E. Daltrozzo, and A. Zumbusch, *Angew. Chem., Int. Ed.* 50, 1406 **(2011)**.
2. S. A. Jenekhe and J. A. Osaheni, *Science* 265, 765 **(1994)**.
3. Z. R. Grabowski and K. Rotkiewicz, *Chem. Rev.* 103, 3899 **(2003)**.
4. P. Bauer, H. Wietasch, S. M. Lindner, and M. Thelakkat, *Chem. Mater*. 19, 88 **(2007)**.
5. G. Sonmez, H. Meng, and F. Wudl, *Chem. Mater.* 15, 4923 **(2003)**.
6. J. Mei, Y. Hong, J. W. Y. Lam, A. Qin, Y. Tang, and B. Z. Tang, *Adv. Mat*. 26, 5429 **(2017)**.
7. R. West, H. Sohn, U. Bankwitz, J. Calabrese, Y. Apeloig, and T. Mueller, *J. Am. Chem. Soc*. 117, 11608 **(1995)**.
8. S. Yamaguchi and K. Tamao, *J. Chem. Soc., Dalton Trans.* 3693 **(1998)**.
9. K. Tamao, M. Uchida, T. Izumizawa, K. Furukawa, and S. Yamaguchi, *J. Am. Chem. Soc.* 118, 11974 **(1996)**.
10. H. Sohn, R. R. Huddleston, D. R. Powell, and R. West, *J. Am. Chem. Soc*. 121, 2935 **(1999)**.
11. Y. Xu, T. Fujino, H. Naito, T. Dohmaru, K. Oka, H. Sohn, and R. West, *Jpn. J. Appl. Phys*. 38, 6915 **(1999)**.
12. Y. H. Park, Y. Kim, and H. Sohn, *J. Korean Phys. Soc*. 59, 2318 **(2011)**.
13. H. Sohn, R. M. Calhoun, M. J. Sailor, and W. C. Trogler, *Angew. Chem. Int. Ed*. 40, 2104 **(2001)**.
14. H. Sohn, M. J. Sailor, D. Magde, and W. C. Trogler, *J. Am. Chem. Soc*. 125, 3821 **(2003)**.
15. J.-K. Choi, S. Jang, K.-J. Kim, H. Sohn, and H.-D. Jeong, *J. Am Chem. Soc*. 133, 7764 **(2011)**.
16. J. Luo, Z. Xie, J. W. Y. Lam, L. Cheng, H. Chen, C. Qiu, H. S. Kwok, X. Zhan, Y. Liu, D. Zhu, and B. Z. Tang, *Chem. Commun.* 1740 **(2001)**.
17. S. Jang, S. G. Kim, D. Jung, H. Kwon, J. Song, S. Cho, Y. C. Ko, and H. Sohn, *B. Kor. Chem. Soc*. 27, 1965 **(2006)**.
18. L. C. Palilis, A. J. Maekinen, M. Uchida, and Z. H. Kafafi, *Appl. Phys. Lett*. 14, 2209 **(2003)**.
19. B.-K. An, S.-K. Kwon, S.-D. Jung, and S. Y. Park, *J. Am. Chem. Soc*. 124, 14410 **(2002)**.
20. M. H. Lee, D. Kim, Y. Dong, and B. Z. Tang, *J. Korean Phys. Soc*. 45, 329 **(2004)**.
21. A. Sekiguchi, S. S. Zigler, and R. West, *J. Am. Chem. Soc*. 108, 4241 **(1986)**.
22. N. J. Turro, Modern Molecular Photochemistry, University Science Books, Sausalito, California **(1991)**.
23. S. J. Toal, D. Magde, and W. C. Trogler, *Chem. Commun.* 5465 **(2005)**.
24. I. Toulokhonova, R. Zhao, M. Kozee, and R. West, *Main Group Metal Chemistry* 24, 737 **(2011)**.

Received: 21 December 2017. Accepted: 18 January 2018.